



Impact of Parameter Variation on Sensorless Indirect Field Oriented Control of Induction Machine

Andrej Kacenska^(✉), Pavol Makys, and Lubos Struharnansky

Faculty of Electrical Engineering, University of Zilina, Žilina, Slovakia
andrej.kacenska@gmail.com,
{pavol.makys, struharnansky}@fel.uniza.sk

Abstract. A method is taken to the control of induction motor based electric drives without the aid of shaft mounted speed or position sensors. This method is called sensorless control. This paper describes a set of three observers used to estimate rotor speed and rotor flux angle which is needed to perform the Park transformation in Indirect Field Oriented Control (IFOC). The validity of the proposed method has been verified by simulation in Matlab and experimentation with frequency inverter controlled by digital signal controller (DSC). The accuracy of the speed estimate relies on the parameters of the machine, such as rotor time constant and stator resistance. These parameters variation causes an estimation error of the motor speed. This error could result in the decrease of control performance. This paper describes the effect of the motor parameters variation on angular velocity estimation.

Keywords: Induction machine · Sensorless indirect field oriented control · Pseudo sliding-mode observer

1 Introduction

Induction machines (IM) are widely used in industry and are adequate for almost any kind of environment. IM provide a wide speed range, high reliability, mechanically robustness, high efficiency and low price. However, induction machines have complex mathematical model, non-linear behaviour due to saturation and parameters variation which depends on the physical influence of temperature. For those reasons is the control of induction machines much more complex.

Since 1990 technology development in power semiconductors, microprocessors and logical programmable devices has made effective controls with adjustable speed feasible [1].

In general, two schemes have been proposed to control induction machines. The first scheme is called Scalar Control (SC). The constant Volt per Hertz ratio represents the scalar control. SC is relatively simple method mainly used in HVAC applications. The second scheme is called Field Oriented Control (FOC). The development of the FOC, induction machine drives became able to provide the same performance as the direct current machine drives. The FOC technique brings overall improvements in drive

performance when compared to the scalar control (full torque control from zero to nominal speed, decoupled control of flux and torque, improved dynamics). With this technique, it is possible to uncouple the stator current components. Uncoupling establishes two independent and single controlled currents. FOC principle is to separate out the component of the stator currents responsible for producing torque and component responsible for producing magnetic flux. The torque component of stator current i_{sq} is similar to armature current of DC motor and the flux component i_{sd} is similar to field current of DC motor. Using these currents, the flux and torque can be independently controlled. In addition, a 90° electric angle is ensured between the uncoupled control currents. As a result, the model of the induction motor loses its complexity, and high drive performance can be realized [2]. The field oriented control ensures good and robust control in case of transients. The principle of field oriented control works with rotating vectors (or phasors) in a complex coordinate system. The magnitude and the phase of the controlled current change. FOC can be carried out by system and coordinate transformations of the basic equations of the motor. After applying the transformations, the alternating and sinusoidal quantities become non-alternating quantities. Due to uncoupling, the currents can be controlled, and then, after back-transformation it is possible to modify the output of the inverter with three-phase quantities. Subsequently, the magnitude and the phase of supplied voltage or current can be modified.

The most common topology for AC drives is based on a Voltage-Source Inverter (VSI) with a rectifier and a DC-link. Generally, the FOC for the induction motor drives can be divided into two categories: indirect and direct schemes. The field to be oriented can be stator, rotor or air-gap flux linkage. In the indirect field oriented control (IFOC) the slip velocity needs to be calculated and rotor speed can be either measured by sensor attached to the rotor or estimated to get synchronous speed. In IFOC scheme rotor flux estimation is not appearing. For the Direct Field Oriented Control (DFOC), the synchronous speed is calculated based on the flux angle, which is obtained from flux estimator or flux sensor.

If in IFOC estimators and/or observers are used to get rotor speed instead of speed sensor attached to the rotor, it can be spoken about sensorless indirect field oriented control. In recent years, a large number of sensorless field oriented control schemes for induction machine have been proposed. Where efficiency, low cost and control of the induction machine drive is a concern, the sensorless IFOC provides the best solution. The term sensorless does not represent the lack of sensors, but it means that speed or position sensor is missing. In IFOC, the speed or position are estimated using other parameters such as phase voltages, currents and IM equivalent circuit parameters. The needlessness of speed sensor decreases both cost and size of induction machine drive. Moreover, this technique is being deployed in hostile environments such as high temperature, corrosive contact, etc. During the last few decades, the sensorless controlled electrical drives has undergone rapid expansion due to the benefits of digital signal controllers. DSC become available allowing to obtain rotor speed by means of observers and estimators integrated with motor control.

In this paper is presented the sensorless Indirect Field Oriented Control of real induction machine. This control method is verified by simulation in Simulink and experimentation with three-phase frequency inverter controlled by DSC TMS320f28062. The effect of motor parameters variation on rotor speed is taken into account.

2 Mathematical Modelling of IM

The mathematical model of the induction motor is used with the consideration of an electromagnetic process in the simulation and experimentations. This mathematical model represents a multi—parameters, non—linear system with the following conclusions, for simplification of the mathematical description [3]:

- The induction machine is symmetrical.
- The air gap is considered to be constant.
- Iron losses can be neglected.
- Resistances and inductances are the same at all phases.

One of the motivations was to eliminate the on-line computation of time varying transformation matrices, as required in conventional field oriented control methods, and for this reason, the basis for the control system development is the following induction motor model, formulated in the stator-fixed (α , β) reference frame. The angular velocity, rotor flux and current differential equations may be expressed as [4]:

$$\dot{\omega}_r = \frac{1}{J}(\Gamma - \Gamma_L) = \frac{1}{J}(c_5 \Psi^T T^T I - \Gamma_L) \quad (1)$$

$$\dot{\Psi} = -P(\omega_r)\Psi + c_4 I \quad (2)$$

$$\dot{I} = c_1 [c_2 P(\omega_r)\Psi - a_1 I + U] \quad (3)$$

where $\Psi^T = [\Psi_\alpha \Psi_\beta]$ is the rotor magnetic flux, $\mathbf{I}^T = [i_\alpha i_\beta]$ is the stator current, $\mathbf{U}^T = [u_\alpha u_\beta]$ is the stator voltage, Γ is the torque developed by the motor, ω_r is the mechanical rotor speed, $c_i, i = 1, 2, 3, 4, 5$ and a_1 are constants, given by: $c_1 = L_r / (L_s L_r - L_m^2)$, $c_2 = L_m / L_r$, $c_3 = R_r / T_r = 1 / T_r$, $c_4 = L_m / T_r$, $c_5 = 3pL_m / 2L_r$, $a_1 = R_s + (L_m^2 + L_r^2)R_r$, where L_s , L_r and L_m are, respectively, the stator and rotor resistances and p is the number of stator pole pairs [4]. Also,

$$\mathbf{P}(\omega_r) = \begin{bmatrix} c_3 & p\omega_r \\ -p\omega_r & c_3 \end{bmatrix} \quad (4)$$

3 State Estimation and Filtering

The rotor magnetic flux, rotor speed and load torque are produced by the following set of three observers. The first is rotor magnetic flux estimator. The second is a stator current vector pseudo sliding—mode observer formulated for generation of an unfiltered estimate of the rotor speed. The third observer provides filtered rotor speed and load torque estimates, a direct measurement of load torque being assumed to be unavailable [4].

3.1 The Rotor Magnetic Flux Estimator

For induction motors a means of estimating the rotor magnetic flux components may be devised by eliminating the rotor speed, ω_r , between Eqs. (2) and (3), yielding Eq. (5) [4].

$$\begin{bmatrix} \Psi_\alpha^* \\ \Psi_\beta^* \end{bmatrix} = \int \left[\left(c_4 - \frac{a_1}{c_2} \right) \begin{bmatrix} I_\alpha \\ I_\beta \end{bmatrix} + \left(\frac{1}{c_2} \right) \begin{bmatrix} U_\alpha \\ U_\beta \end{bmatrix} \right] dt - \left(\frac{1}{c_1 c_2} \right) \begin{bmatrix} I_\alpha \\ I_\beta \end{bmatrix} \tag{5}$$

With zero initial conditions, all the quantities on the right side of Eq. (5) are known, but the pure integration would be subject to drift in practice. This problem is overcome here by noting that $\int_0^\infty \Psi(t)dt = 0$. Accordingly, if $\|\Psi\|$ exceeds $(1 + \lambda)\|\Psi\|_d$ where $0 < \lambda < 1$, the drift is prevented by replacing the integral of Eq. (5) by first order filter with a time constant, T_q such that $T_q \gg 1/\omega_{rmin}$ is the lowest angular velocity envisaged for the particular application [4].

3.2 The Pseudo Sliding Mode Observer and Angular Velocity Extractor

A stator current pseudo—sliding—mode observer is formulated for generation of an unfiltered estimate, $c_1 c_2 P(\widehat{\omega}_r) \widehat{\Psi}$, of the term, $c_1 c_2 P(\omega_r) \Psi$. The observer is therefore formed as a stator current real time model purposely omitted terms containing ω_r . Thus:

$$\dot{\mathbf{I}}^* = c_1 [-a_1 \mathbf{I}^* + \mathbf{U}] - \mathbf{v} \tag{6}$$

$$\mathbf{v} = -v_{max} \cdot \text{sgn}[\mathbf{I}^* - \mathbf{I}] \tag{7}$$

Where $\mathbf{v}^T = [v_\alpha \ v_\beta]$ are the model corrections, i_α^* and i_β^* are estimates of i_α and i_β , as in conventional observers. The useful observer output here, however, are the continuous equivalent values \mathbf{v}_{eq} , of the rapidly switching \mathbf{v} . But Eq. (7) cannot directly generate the equivalent values. Instead, a pseudo—sliding—mode observer may be formed by replacing the signum function by high gain.

$$\mathbf{v}_{eq} = K_{SM}[\mathbf{I}^* - \mathbf{I}] \tag{8}$$

Where K_{SM} is a high gain so that \mathbf{v} is continuous and closely approaches \mathbf{v}_{eq} for sufficiently high gain, limited only by the non-zero iteration interval, h , of the digital implementation $K_{SM} < (2 - c_1 a_1 h)/h$ with Euler explicit numerical integration. The resulting approximation to \mathbf{v}_{eq} is denoted \mathbf{v}_{eq}^* . Assuming that observer operates in the ideal sliding mode, $\mathbf{v} = \mathbf{v}_{eq}$ if $\mathbf{I}^* = \mathbf{I}$ and $\dot{\mathbf{I}}^* = \dot{\mathbf{I}}$. Then the right sides of Eqs. (3) and (6) may be equated, yielding (with \mathbf{v}_{eq} replaced by \mathbf{v}) [4]:

$$c_1 [-a_1 \mathbf{I}^* + \mathbf{U}] - \mathbf{v}_{eq}^* = c_1 [c_2 P(\omega_r) \Psi - a_1 \mathbf{I} + \mathbf{U}] \tag{9}$$

Replacing Ψ and ω_r in Eq. (9) by their estimates Ψ^* and ω_r^* yields:

$$\mathbf{v}_{\text{eq}}^* = -c_1 c_2 P(\omega_r^*) \Psi^* \quad (10)$$

The following formula for the desired angular velocity estimate ω_r^* is then derived from the components, \mathbf{v}_{eq}^* of Eq. (10):

$$\omega_r^* = \frac{-v_{\text{eq}\alpha}^* \Psi_{\beta}^* + v_{\text{eq}\beta}^* \Psi_{\alpha}^*}{c_1 c_2 p \|\Psi^*\|} \quad (11)$$

3.3 Observer for Load Torque Estimation and Rotor Speed Estimate Filtering

The real time model of this observer is based on motor torque equation. The load torque is treated as a state variable whose differential equation augments the real time model. In this case, the load torque is assumed constant in the formulation of the real time model and so its state differential equation is simply $\dot{\Gamma}_L = 0$. The observer correction loop is actuated by the error between the rotor speed estimate, ω_r^* , and the filtered estimate, $\widehat{\omega}_r$, from the real time model. Since, $\widehat{\omega}_r$ is a filtered version of ω_r^* , it is used directly in the control loop instead of ω_r^* . The continuous time version of this observer is therefore [4]:

$$\mathbf{e}_{\omega} = \omega_r^* - \widehat{\omega}_r \quad (11)$$

$$\frac{d\widehat{\omega}_r}{dt} = \frac{1}{J} \left[c_5 (\Psi_{\alpha} i_{\beta} - \Psi_{\beta} i_{\alpha}) - \widehat{\Gamma}_L \right] + k_{\omega} \mathbf{e}_{\omega} \quad (12)$$

$$-\frac{d\widehat{\Gamma}_L}{dt} = k_{\Gamma} \mathbf{e}_{\omega} \quad (13)$$

The observer poles are both placed at $s = -1/T_f$ so that the filtering time constant, T_f , is a single design parameter for the gains, k_{ω} and k_{Γ} as it is shown in (15), where the right side of equation is the characteristic equation of the filtering observer characteristics polynomial [4]:

$$s^2 + \frac{2}{T_f} s + \frac{1}{T_f^2} = s^2 + k_{\omega} s + \frac{k_{\Gamma}}{J} \quad (15)$$

$$k_{\omega} = \frac{2}{T_f} \quad k_{\Gamma} = \frac{J}{T_f^2} \quad (16)$$

4 Simulation

Simulation has been realized using software product Matlab-Simulink to verify a validity of proposed sensorless IFOC method. Control structure is shown in Fig. 1. Set of three above mentioned observers has been used to get rotor velocity estimate.

Table 1. Parameters of the investigated IM

Sign	Definition	Value	Unit
P_N	Rated power	1.5	kW
U_N	Rated voltage	400	V
I_N	Rated current	3.4	A
J	Rotor moment of inertia	0.0035	$kg \cdot m^{-2}$
R_S	Stator winding resistance	5.155	Ω
R_r	Rotor winding resistance	4.426	Ω
L_S	Stator winding inductance	0.291	H
L_r	Rotor winding inductance	0.291	H

This velocity estimate has been used as a feedback signal in speed control loop. The coefficients of PI controller have been tuned by trial and error method [5].

In simulation we use the induction machine parameters as shown in Table 1. The demanded magnetic flux is set 1.5 Wb and demanded angular velocity is set to 157 rad/s. The simulation results are shown in Fig. 2, 3 and 4.

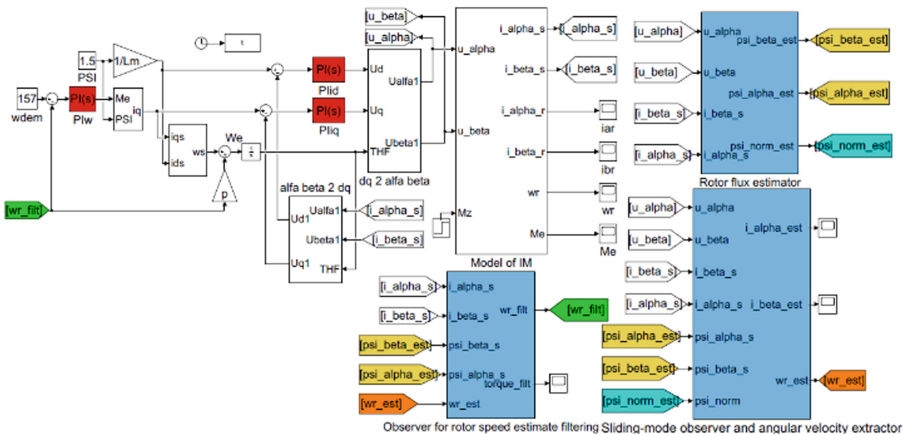


Fig. 1. A simulation model.

In Fig. 2, can be seen comparison of both rotor angular velocity and the rotor angular velocity estimate. The start up of IM has been simulated under no load conditions and since time 0.5 s load torque has been kept constant at rated value 10.1 Nm. In Fig. 2 can be also seen the difference between rotor angular velocity and rotor angular velocity estimate at steady state. It is approximately 1.9 rad/s at both no-load conditions and at rated load torque.

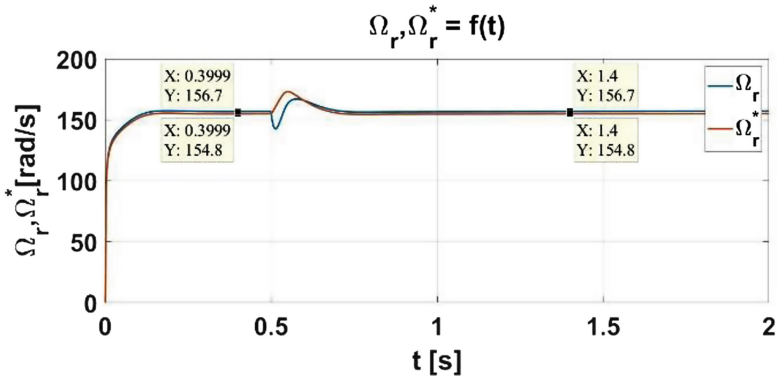


Fig. 2. Simulated rotor speed and rotor speed estimate

Figure 3 shows rotor flux expressed as a square of rotor flux estimates magnitudes.

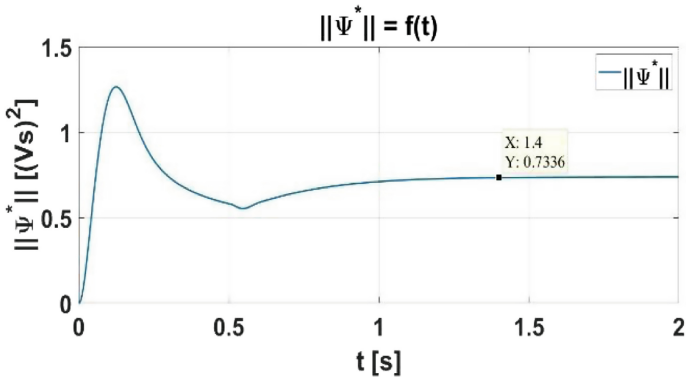


Fig. 3. Simulated rotor flux norm

In the Fig. 4, there are shown motor currents for start up and steady state. Current i_α is α -component of stator current and current i_α^* is its estimated value.

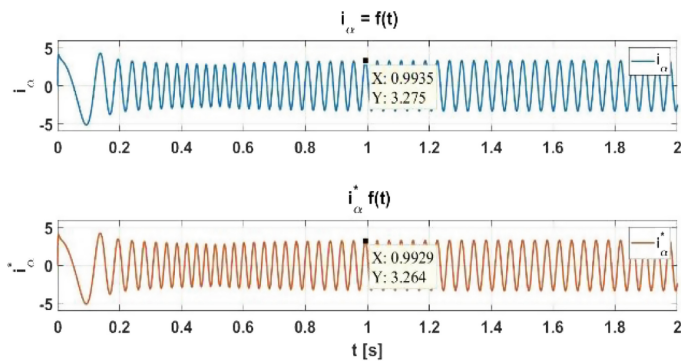


Fig. 4. Simulated α -component current and its estimate

5 Experimental Results

To verify the proposed method and simulation results an experimental stand with IM coupled with dynamometer as a load has been used. The experiments were performed with 1.5 kW induction machine powered by three-phase frequency inverter as shown in Fig. 5. Table 1 gives the machine parameters. The control law was implemented via Digital Signal Controller TMS320f28062 by Texas Instruments. The switching frequency was set as 10 kHz. The coefficients of PI controller have been tuned by trial and error method and by Ziegler-Nichols method.

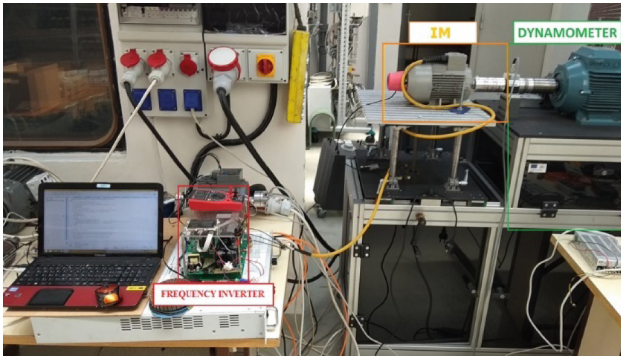


Fig. 5. Experimental stand equipped with IM and dynamometer

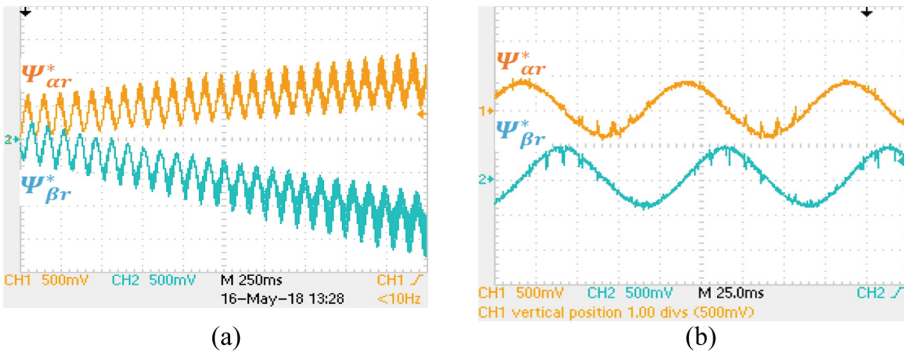


Fig. 6. The estimated rotor flux components before filtering (a) and after filtering (b)

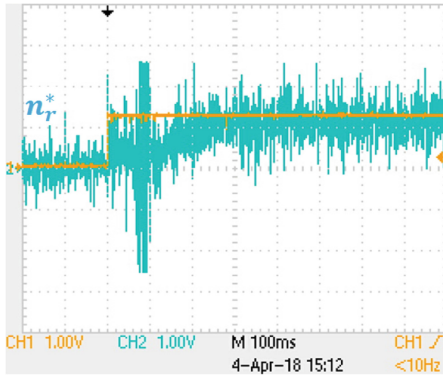


Fig. 7. The unfiltered rotor speed estimate

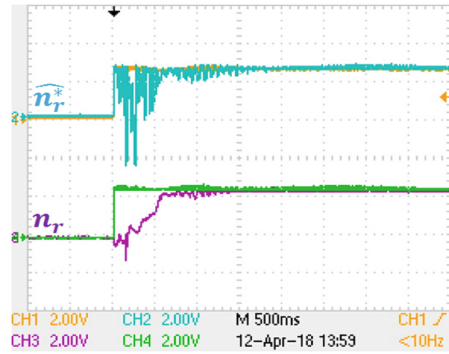


Fig. 8. The filtered rotor speed estimate and actual rotor speed

In the Fig. 6, there are shown estimated rotor flux components both before filtering (a) and after filtering (b). The pure integration of the Eq. (5) is a subject to drift in practice as shown in (a). To eliminate this drift the first order filter with time constant $t_q = 0.15$ s has been applied.

In the Fig. 7 is shown step response of unfiltered rotor speed estimate at start up, where demanded speed is 500 rpm. In the Fig. 8 is shown step response of filtered rotor speed estimate (blue colour) and actual rotor speed measured by encoder (purple colour) at start up, where demanded speed is 500 rpm.

6 The Effect of Machine Parameters Error on Rotor Speed Estimation

In Indirect Field Oriented Control and mainly in sensorless IFOC which utilizes a set of observers presented in this paper to get rotor speed estimate, equivalent circuit parameters need to be known.

These parameters are not constant and may differ in a wide range from operating point to another operating point i.e. these parameters are affected by temperature, saturation, frequency and skin effect [6]. The machine parameters used in sensorless IFOC includes the stator inductance, rotor inductance, stator resistance and rotor resistance, L_s , L_r , R_s , R_r , respectively.

Especially, a winding temperature can vary a lot during operation, resulting winding resistances mismatch. This mismatch influence on rotor speed estimation has been analysed in this paper. To emulate resistances mismatch, the incorrect parameters in digital signal controller have been set. One of the most important tasks of DSC is to calculate rotor speed both from the mathematical model of IM and from mathematical model of observers in a real time. Described models utilize winding resistance as a

parameter and are highly sensitive to its error [7]. If the assumed values of resistances are not consistent with real ones, rotor speed is not correctly estimated.

6.1 The Effect of Rotor Resistance Error on Speed Estimation

First of all, the effect of rotor resistance error on rotor speed estimate has been investigated. Rotor resistance is a parameter which is important both in sensed IFOC and in sensorless IFOC in order to calculate slip frequency (Fig. 9).

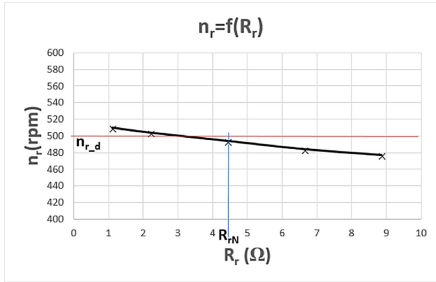


Fig. 9. The rotor speed versus rotor resistance

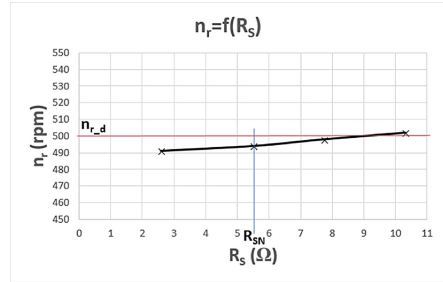


Fig. 10. The rotor speed versus stator resistance

As shown in Fig. 10, with the proposed sensorless IFOC scheme, the rotor speed decreases from 510 rpm to 477 rpm as rotor resistance increases from $0.25R_{rN}$ to $2R_{rN}$. The speed reference is set as 500 rpm. It can be seen, that there is also a deviation between reference speed and actual speed at rated rotor resistance due to incorrect equivalent circuit parameters determination.

6.2 The Effect of Stator Resistance Error on Speed Estimation

Another parameter being analysed is a stator resistance. It has a strong influence on speed estimation in sensorless IFOC drive but contrary to IFOC with sensor on the shaft its influence can be neglected [8]. As shown in Fig. 10, the rotor speed increases from 491 rpm to 502 rpm as stator resistance increases from $0.5R_{sN}$ to $2R_{sN}$. The speed reference is set as 500 rpm. It can be seen, that there is also a deviation between reference speed and actual speed at rated stator resistance due to incorrect equivalent circuit parameters determination.

7 Conclusion

This paper has presented the sensorless Indirect Field Oriented Control in Induction Machine drive. A set of three observers needed to estimate rotor velocity has been described. The validity of proposed method has been verified by simulation in Simulink and experimentation with frequency inverter controlled by DSC. Speed estimation

applying set of described observers has led to inaccuracy due to motor parameters mismatch. The effect of rotor and stator resistance variation on the performance of the sensorless indirect field oriented control has been also investigated. The results indicate that when the parameters are inaccurate, the actual rotor speed diverges from the command. It is to be highlighted, that rotor resistance error has stronger influence on rotor speed variation.

Acknowledgment. This work was supported by Slovak Scientific Grant Agency VEGA No. 1/0774/18. and by project ITMS: 26220120046, co-funded from EU sources and European Regional Development Fund.

References

1. Rodríguez-Reséndiz, J, Rivas-Araiza E., Herrera-Ruiz, G.: Indirect field oriented control of an induction machine sensing DC-link current. In: IEEE Electronics, Robotics and Automotive Mechanics Conference (2008)
2. Kohlrusz, G., Fodor, D.: Comparison of scalar and vector control strategies of induction motors University of Pannonia, Faculty of Engineering (2011)
3. Brandstetter, P., Kuchar, M.: Rotor flux estimation using voltage model of induction motor. Technical University of Ostrava (2015)
4. Vittek, J., Dodds, J.S.: Forced dynamics control of electric drives (2003)
5. Kacenkova, V., Rafajdus, P., Makys, P., Vavrus, V., Szabo, L.: Static and dynamic fault analysis of switched reluctance motor. University of Zilina, Faculty of Electrical Engineering (2012)
6. Soliman, H.M.: Effect of the parameters variation for induction motor on its performance characteristics with field oriented control compared to scalar control (2016)
7. Timer, J., Adzic, E., Porobic, V., Marcetic, D.: Influence of rotor time constant error on IFOC control structure (2009)
8. Dumnic, B., Ivanovic, Z., Katic, V., Vasic, V., Delimar, M.: Sensorless vector control and effects of machine parameters mismatch in variable speed wind turbines (2007)